



PEARL

**Resuspension of microplastics and microrubbers in a semi-arid urban environment (Shiraz, Iran)**

Khodabakhshloo, Nafiseh; Abbasi, Sajjad; Turner, Andrew

**Published in:**  
Environmental Pollution

**DOI:**  
[10.1016/j.envpol.2022.120575](https://doi.org/10.1016/j.envpol.2022.120575)

**Publication date:**  
2023

**Link:**  
[Link to publication in PEARL](#)

**Citation for published version (APA):**  
Khodabakhshloo, N., Abbasi, S., & Turner, A. (2023). Resuspension of microplastics and microrubbers in a semi-arid urban environment (Shiraz, Iran). *Environmental Pollution*, 316(0). <https://doi.org/10.1016/j.envpol.2022.120575>

All content in PEARL is protected by copyright law. Author manuscripts are made available in accordance with publisher policies. Wherever possible please cite the published version using the details provided on the item record or document. In the absence of an open licence (e.g. Creative Commons), permissions for further reuse of content should be sought from the publisher or author.



11 **Abstract**

12 Although airborne urban particulates are a concern for air quality and human health, little  
13 information exists on the levels and characteristics of microplastics (MPs) and microrubbers  
14 (MRs) in this setting. In the present study, MPs and MRs are quantified and characterised in road  
15 dusts and accumulations captured passively (and up to elevations of about 1.8 m above road  
16 level) in the steps of utility poles at 18 locations throughout the city of Shiraz, southwest Iran.  
17 Dust accumulation rates were greatest at road level (median =  $45 \text{ g m}^{-2} \text{ month}^{-1}$ ) and declined  
18 with elevation (median =  $2.0 \text{ g m}^{-2} \text{ month}^{-1}$  at 177 cm). The concentrations (per g of dust) and  
19 accumulation of MPs and MRs were more variable between locations but accumulation declined  
20 with elevation for both particle types and MR concentration (up to  $\sim 27,000 \text{ MR g}^{-1}$ ) was always  
21 greater than corresponding MP concentration (up to  $\sim 3300 \text{ MP g}^{-1}$ ). Increasing elevation was  
22 also accompanied by an increasing proportion of fine ( $\leq 100 \mu\text{m}$ ) and fibrous particles, and in  
23 particular for MPs. Fractionation in the quantities and characteristics with elevation above road  
24 level are attributed to the extent of resuspension of MPs and MRs from the road surface by wind  
25 and passing traffic, with aerodynamic considerations predicting the greatest and most widespread  
26 resuspension of fibrous MPs. The fractionation of MPs and MRs with elevation above road level  
27 also result in different exposures for adults and children.

28

29 **Keywords:** dusts; street; aerodynamic; exposure; accumulation; fibres

30

31

## 32 **1. Introduction**

33 Road dust is a heterogeneous reservoir of particulate matter arising from various sources,  
34 including abrasion of the road surface and mechanical vehicle components, exhaust emissions  
35 from traffic, and deposition of regional airborne geogenic and biogenic particles (Thorpe and  
36 Harrison, 2008). In turn, settled road dust represents a secondary source of airborne particulate  
37 matter when fine particles are resuspended back into the local atmosphere through wind and  
38 passing vehicles, and especially under dry conditions (Rogge et al., 1993; Panko et al., 2013;  
39 Fussell et al., 2022).

40 In urban environments, resuspension of road dust is an increasing concern for air quality and  
41 human health. With vehicle exhaust emissions being progressively regulated, it has been  
42 suggested that resuspension is at least as significant to the population of particles having  
43 aerodynamic diameters less than 10  $\mu\text{m}$  ( $\text{PM}_{10}$ ) and for respiratory and cardiovascular health as  
44 exhaust sources (Kuenan et al., 2014; Weinbruch et al., 2014; Thouron et al., 2018). As a  
45 consequence, there have been attempts to empirically model road dust emissions and exposures,  
46 but this is often hampered by a lack of knowledge of the resuspension process itself, and the  
47 complex effects of different vehicle categories, driving behaviours, road surfaces and climates on  
48 emissions (Ventrakam, 2000; Escrig et al., 2011). As an alternative, emissions have also been  
49 estimated more directly through mass balance calculations and the measurement of source  
50 materials or tracers collected by passive sampling devices deployed at different elevations above  
51 the street surface (Wagner and Leith, 2001; Amato et al., 2012).

52 Particles from tyre wear, largely made up of natural and synthetic rubbers, have been recognized  
53 as an important contributor to road dust in the urban setting (Alvez et al., 2020; Moskovchenko  
54 et al., 2022). However, relatively little quantitative information exists on their abundance,  
55 through direct microscopic imagery or via some chemical marker of tire tread, for example, or  
56 their resuspension from the road surface (Abbasi et al., 2019; Panko et al., 2019; Youn et al.,  
57 2021). Moreover, and despite the ubiquity of microplastics (MPs, and comprising synthetic,  
58 petroleum-based polymers) and the extensive literature addressing their importance in the  
59 atmosphere (Dris et al., 2016; Liu et al., 2019; Brahney et al., 2020; Abbasi et al., 2022), even  
60 less information exists on their occurrence in road dusts (Abbasi et al., 2019; Järskog et al.,  
61 2020; O'Brien et al., 2021). Significantly, and as far as we are aware, there has been no

62 consideration of MPs in relation to their resuspension from a road surface as a secondary, urban  
63 source.

64 In the present study, we consider both MPs and microrubbers (MRs, and dominated by tire wear  
65 particulates) in road dusts and material sampled passively at different elevations above street  
66 level in Shiraz, a large, semi-arid city in southwest Iran. MPs and MRs are identified,  
67 discriminated and characterised by established techniques and differences in particle  
68 characteristics as a function of elevation are used to infer information about their sources,  
69 resuspension from the road surface and potential for human exposure in the urban setting.

70

## 71 **2. Materials and methods**

### 72 **2.1. Study area and sample collection**

73 Sampling was undertaken within the Shiraz metropolitan district of southwest Iran (population ~  
74 2 M). Urbanized Shiraz covers an area of about 240 km<sup>2</sup> that lies on the plain of a seasonal river  
75 with underlying sedimentary rocks at an elevation of about 1600 m above sea level. The climate  
76 is moderate semi-arid, with an annual average rainfall and temperature of 335 mm and 18 °C,  
77 respectively, and a prevailing wind from the north to north-west (average annual wind speed is  
78 2.35 m s<sup>-1</sup>).

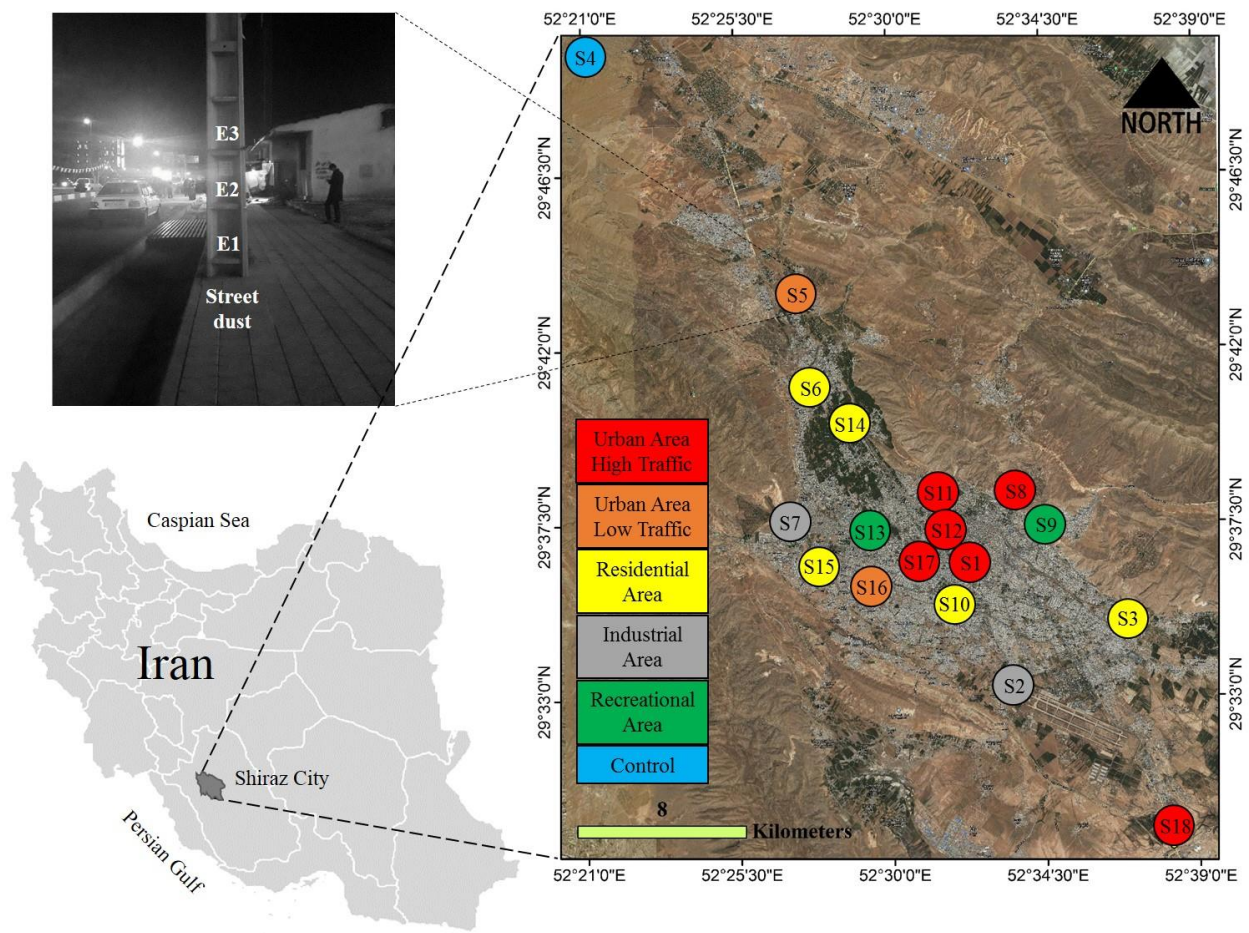
79 Air pollution in Shiraz results from primitive forms of heating, traffic, agriculture and various  
80 manufacturing, processing and refining industries (mainly related to cement and oil production  
81 and energy generation). Air quality in the city has been declining over recent years because of  
82 growth in population and urbanization and an increasing incidence of dust storms (Abbasi et al.,  
83 2022).

84 Sampling was conducted during the dry season in 2021 at 17 sites within different municipal  
85 sectors of Shiraz (urban, residential, industrial-commercial, recreational) and at a control location  
86 to the northwest and upwind of the city and at an altitude of about 1900 m above sea level (Ghalat  
87 (Figure 1). At each site, the three lower steps (or 485 cm<sup>2</sup> cavity floors) of a 12-m concrete utility  
88 pole (at elevations of 23 cm, 101 cm and 177 cm above the pavement) and a semicircular 1570  
89 cm<sup>2</sup> area of the (asphalt) road surface adjacent to the kerb were cleaned using distilled water and  
90 with the aid of a pre-cleaned horsehair wooden brush in May (Figure 1). During October, and a

91 after a passive sampling period of about 150 days, the sites were re-visited and material that had  
92 accumulated over the five-month period was transferred onto individual sheets of aluminium foil  
93 with the aid of the brush and a stainless steel dustpan. Any visible debris, including leaves,  
94 cigarette butts and pieces of paving stone, asphalt, concrete and brick, were manually removed  
95 before the contents were carefully wrapped and sealed.

96

97



98

99

100 Fig 1. Sampling locations and their municipal categorisation in Shiraz, southwest Iran. The  
101 photograph shows a concrete utility pole and the lower three steps (E1, E2 and E3) used for  
102 passive sampling

103

104 **2.2. MP and MR isolation**

105 For the isolation, identification and characterisation of MPs and MRs in the dusts, we followed  
106 previously published methods and quality assurance protocols with some modifications (Abbasi  
107 et al., 2017, Abbasi et al., 2019). Briefly, samples ( $n = 72$ ) were sieved through a 5-mm metal  
108 mesh, with fractionated material weighed on a Libror AEL-40SM balance (Shimadzu, Kyoto).  
109 Fractionated material (between about 10 and 100 g of street dust and 0.1 to 5 g of utility pole  
110 dust), plus four controls (in the absence of weighted material), was mixed with 100 to 200 mL of  
111 35% filtered  $H_2O_2$  (Arman Sina, Tehran) for several days (and until bubble formation ceased) in  
112 a series of covered, glass 50 mL beakers. Remaining  $H_2O_2$  was removed by evaporation in a sand  
113 bath at  $50^\circ C$  before 50 mL of filtered, saturated  $ZnCl_2$  solution (Arman Sina, Tehran) was added  
114 to each beaker. The contents were agitated for 5 min at 350 rpm and then allowed to settle for 90  
115 min. Supernatants were centrifuged for 3 min at 4000 rpm before being vacuum-filtered through  
116 S&S filter papers (blue band, grade 589/3, 2  $\mu m$  pore size) and washed with distilled water. The  
117 process of settling, centrifuging, and filtering was repeated three times through the same filter  
118 and dried filters were stored in individual, sealed petri dishes.

119

## 120 **2.3. MP and MR analysis**

121 Whole filters or precisely measured fractions thereof were observed under a stereo digital  
122 microscope (Sairan DSM3000) at 200 x magnification with the aid of ImageJ software. MPs  
123 were identified by their hardness, gloss, uniform thickness and reaction to a hot needle (Hidalgo-  
124 Ruz et al., 2012), while MRs were identified by their distinctively non-glossy, black appearance,  
125 high elasticity and propensity to reversibly deform (Abbasi et al., 2019). MPs and MRs were  
126 classified according to shape as: fiber, film, fragment or spherule; size in terms of length or  
127 primary diameter,  $L$ , as: fine ( $L \leq 100 \mu\text{m}$ ), intermediate ( $100 < L \leq 1000 \mu\text{m}$ ) or coarse ( $L >$   
128  $1000 \mu\text{m}$ ); and, for MP fibres, thickness or diameter,  $d$ , as: thin ( $\leq 10 \mu\text{m}$ ), medium ( $10 < d \leq 20$   
129  $\mu\text{m}$ ) and thick ( $d > 30 \mu\text{m}$ ).

130  
131 The polymeric composition of a selection of MPs from different locations and of different sizes  
132 and shapes ( $n = 30$ ) was determined using a micro-Raman spectrometer (LabRAM HR, Horiba,  
133 Japan) with a laser of 785 nm, a Raman shift of 400–1800  $\text{cm}^{-1}$  and acquisition times between 20  
134 and 30 s.

## 136 **3. Results**

### 137 **3.1. Accumulation of dust**

138 The net accumulation rates of material (dust) at each location and elevation in Shiraz are shown  
139 in Table 1. Here, rates were calculated at E0 (road level) and E1, E2 and E3 (23 cm, 101 cm and  
140 177 cm above the pavement, respectively, and within cavities of the utility poles) from the mass  
141 of material accumulated over a specific area for a period of about 150 days.

142 Inter-location variations in deposition rates are evident at all levels; for example, deposition at  
143 road level ranges from about  $16 \text{ g m}^{-2} \text{ month}^{-1}$  in an urban setting subject to high traffic flow (S1)  
144 to  $120 \text{ g m}^{-2} \text{ month}^{-1}$  in a residential area (S10). Variations likely reflect the complex interplay of  
145 a number of factors relating to the proximity and significance of local dust sources, land use,  
146 microclimate and effects of any buildings on such, topography, surface roughness and road and  
147 utility pole orientation relative to wind direction. By contrast, variations in accumulation rates as  
148 a function of elevation are more consistent amongst different locations and there were no



149 differences that could be attributable to utility pole orientation. Thus, in all but two cases, rates  
 150 were greatest at street level (E0); at ten locations, rates declined progressively with increasing  
 151 elevation, and at all locations, the lowest rates were observed at the greatest elevation (ranging  
 152 from < 0.1 to 6.6 g m<sup>-2</sup> month<sup>-1</sup>).

153

154 Table 1: Net accumulation rates of material at road level and at different elevations for each  
 155 location.

156

location	accumulation, g m <sup>-2</sup> month <sup>-1</sup>			
	E0	E1	E2	E3
S1	16.1	1.9	3.6	0.2
S2	77.6	1.9	2.3	1.1
S3	48.7	8.8	3.4	0.4
S4	52.6	7.3	1.6	1.1
S5	31.4	7.8	12.2	5.1
S6	34.5	7.1	5.0	3.1
S7	43.7	6.2	3.0	3.0
S8	51.2	6.8	12.3	1.4
S9	45.3	23.0	12.9	6.1
S10	118.1	3.4	1.4	1.1
S11	36.2	19.3	9.0	2.6
S12	21.0	21.5	10.3	5.6
S13	63.6	5.7	7.1	5.3
S14	58.5	10.5	13.5	6.6
S15	66.1	3.6	0.2	<0.1
S16	44.7	2.1	1.5	1.0
S17	32.3	34.2	17.9	1.1
S18	23.5	3.1	0.1	<0.1
median	45.0	6.9	4.3	2.0

157

158 Table 2: Abundance and net accumulation rates (mo = month) of MPs and MRs at road level and the different elevations sampled at  
 159 each location. Note, insufficient material was obtained for E3 at S15 and S18 and that median values exclude the corresponding  
 160 control measurements (at S4).

location	E0				E1				E2				E3			
	MP g <sup>-1</sup>	MP m <sup>-2</sup> mo <sup>-1</sup>	MR g <sup>-1</sup>	MR m <sup>-2</sup> mo <sup>-1</sup>	MP g <sup>-1</sup>	MP m <sup>-2</sup> mo <sup>-1</sup>	MR g <sup>-1</sup>	MR m <sup>-2</sup> mo <sup>-1</sup>	MP g <sup>-1</sup>	MP m <sup>-2</sup> mo <sup>-1</sup>	MR g <sup>-1</sup>	MR m <sup>-2</sup> mo <sup>-1</sup>	MP g <sup>-1</sup>	MP m <sup>-2</sup> mo <sup>-1</sup>	MR g <sup>-1</sup>	MR m <sup>-2</sup> mo <sup>-1</sup>
S1	120.6	1936.3	770.3	12366.9	690.0	1323.7	8432.9	16177.3	122.8	445.4	729.1	2643.3	708.0	132.0	1150.4	214.4
S2	119.2	9248.4	728.3	56501.9	1719.3	3233.0	5375.0	10107.2	1770.2	4041.2	850.8	1942.3	154.1	173.2	231.1	259.8
S3	40.5	1972.0	165.0	8040.8	479.0	4210.3	1206.1	10602.1	915.0	3092.8	790.5	2672.2	143.9	57.7	20.6	8.2
S4	0.7	35.7	1.5	79.0	1.1	8.2	6.8	49.5	12.7	20.6	12.7	20.6	0	0	0	0
S5	3.2	99.4	397.2	12458.6	14.7	115.5	743.5	5822.7	4.7	57.7	18.2	222.7	4.0	20.6	10.5	53.6
S6	70.2	2421.7	808.9	27913.4	378.2	2696.9	1509.4	10762.9	952.6	4771.1	7421.4	37171.1	155.9	482.5	56.0	173.2
S7	38.5	1682.8	68.1	2975.8	67.7	420.6	531.4	3303.1	47.1	140.2	94.3	280.4	11.0	33.0	16.4	49.5
S8	82.8	4238.2	799.2	40922.3	172.8	1167.0	3850.0	25995.9	106.4	1307.2	191.6	2354.6	59.9	86.6	376.7	544.3
S9	124.4	5631.8	978.8	44305.7	44.2	1014.4	199.0	4569.1	133.6	1723.7	185.3	2391.8	36.6	222.7	41.3	251.5
S10	24.2	2857.3	192.9	22777.1	105.7	358.8	2164.2	7348.5	722.0	1018.6	926.6	1307.2	40.6	45.4	77.6	86.6
S11	135.3	4894.3	931.1	33671.3	64.2	1241.2	2688.0	51991.8	193.9	1736.1	402.1	3600.0	49.9	132.0	656.8	1736.1
S12	181.0	3805.1	836.8	17589.8	96.2	2066.0	1659.5	35645.4	300.3	3096.9	633.5	6532.0	178.6	993.8	16.3	90.7
S13	17.3	1101.9	292.8	18608.9	81.1	461.9	1739.6	9901.0	56.6	404.1	587.8	4193.8	23.2	123.7	66.4	354.6
S14	34.6	2021.7	181.0	10588.5	155.7	1628.9	607.5	6354.6	20.5	276.3	105.5	1422.7	23.8	156.7	5.0	33.0
S15	24.2	1597.5	200.6	13253.5	621.3	2235.1	3020.4	10866.0	3338.3	828.9	7573.5	1880.4				
S16	44.1	1969.4	315.7	14109.6	167.0	358.8	11556.6	24828.9	414.6	630.9	2945.8	4482.5	77.6	74.2	107.8	103.1
S17	80.2	2588.5	951.4	30726.1	77.2	2643.3	878.2	30070.1	50.6	903.1	50.1	894.8	429.3	461.9	161.0	173.2
S18	135.8	3188.5	670.6	15740.1	151.3	461.9	3837.6	11715.5	1645.6	214.4	27025.3	3521.6				
161 median*	70.2	2421.7	670.6	17589.8	151.3	1241.2	1739.6	10762.9	193.9	903.1	633.5	2391.8	59.9	132.0	66.4	173.2

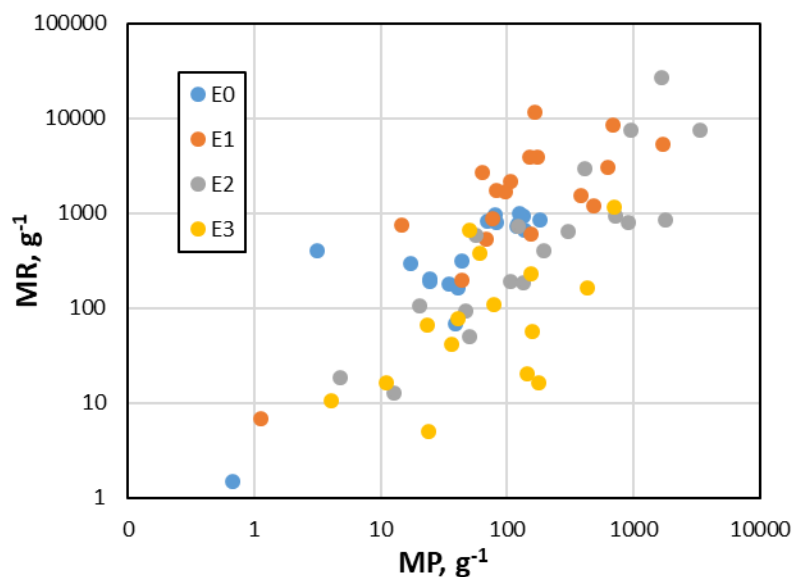
162

163 **3.2. Accumulation of MPs and MRs**

164 The abundance (per g of sample) and net accumulation rates (per m<sup>2</sup> per month) of MPs and  
165 MRs are shown at each elevation for all locations in Table 2. The values of all measures except  
166 for MP abundance at E2 were lowest at the control site, with maximum values at each elevation  
167 at least two orders of magnitude greater than corresponding controls and encountered across all  
168 municipal categories of Shiraz shown in Figure 1 except for urban areas with low traffic. Median  
169 values (excluding control data) are shown as measures of central tendency after it was  
170 established that most data sets were non-normally distributed.

171 According to a series of Wilcoxon signed rank tests performed in Minitab v19, MP abundance  
172 was significantly greater ( $p < 0.05$ ) at E1 and E2 than at E0 and E3, and MP accumulation was  
173 significantly greater at E0 than the remaining elevations. Wilcoxon tests also established  
174 significantly greater medians in MR abundance and accumulation rates than in corresponding  
175 MP abundance and accumulation rates at E0, E1 and E2, but no significant differences between  
176 particle types were observed in either measure at E3.

177



178

179 Figure 2: Abundance of MRs versus abundance of MPs and grouped by elevation.

180

181 Figure 2 is a scatter plot of the abundance of MRs against the abundance of MPs. Overall, and  
182 for each elevation, data were significantly related ( $p < 0.05$ ) according to Pearson's moment  
183 correlation, with equivalent analyses of MRs and MPs on an accumulation basis resulting in  
184 significant, albeit weaker correlations. Median ratios of MR to MP abundance (or measures of  
185 the slopes of the relationships in Figure 2) were about 15 at E0 and E1, but decreased to about 4  
186 and 2.3 at E2 and E3, respectively.

### 187 3.3. Characteristics of MPs and MRs

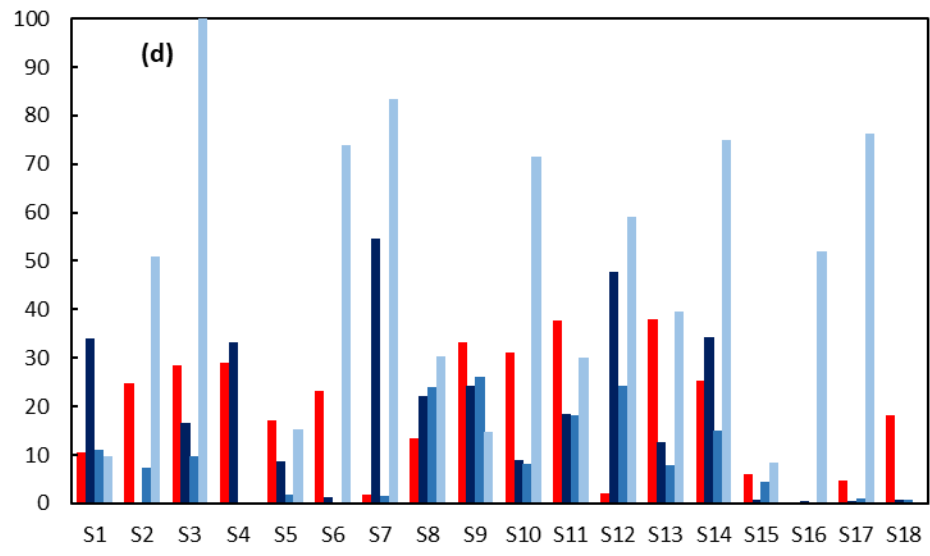
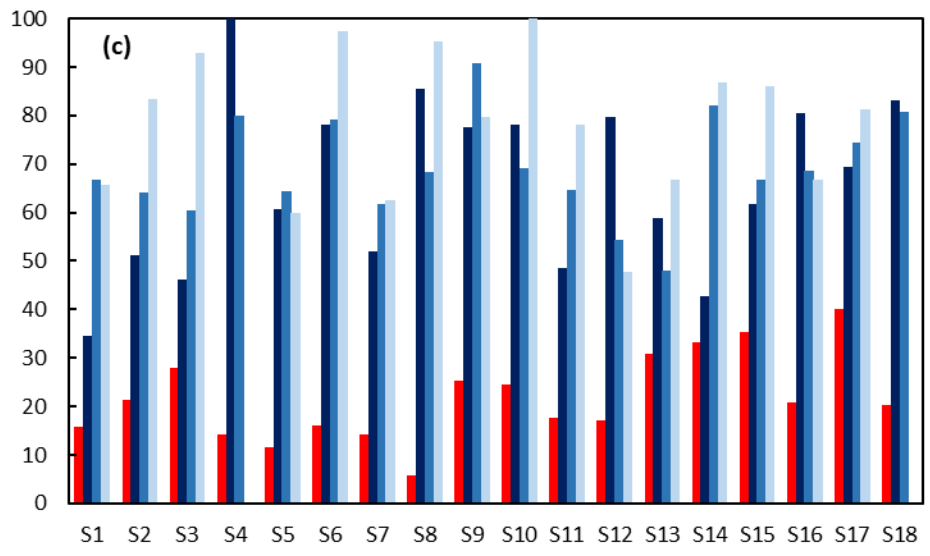
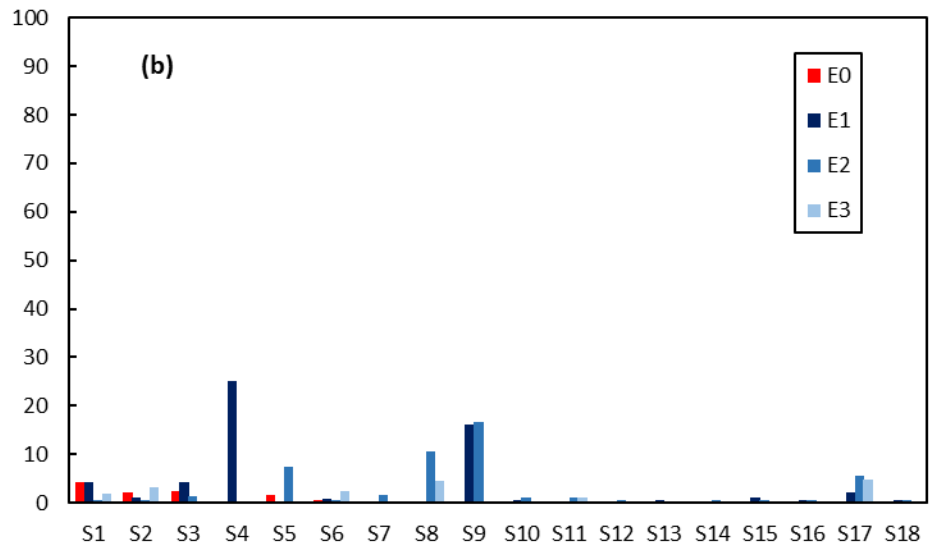
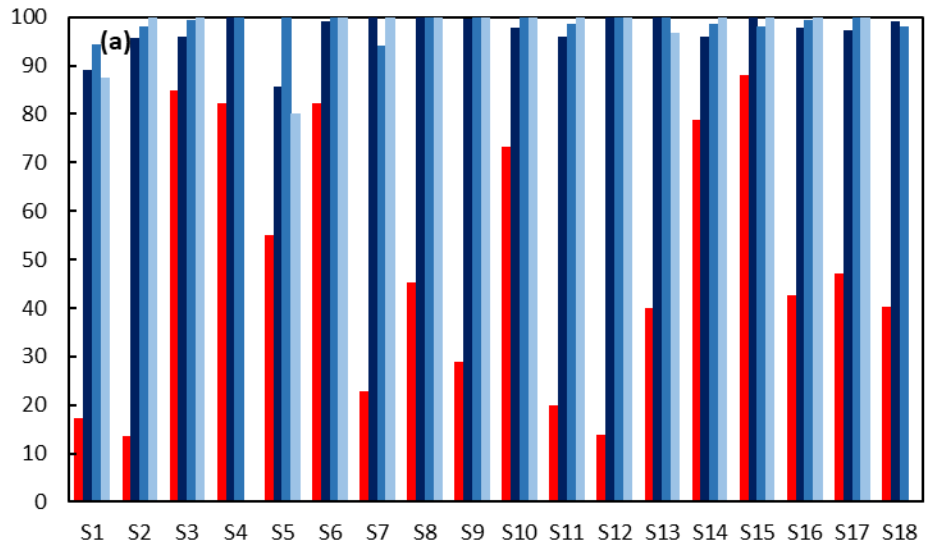
188 The distribution of MPs and MRs by shape and size at each location and elevation is illustrated  
189 in Figure 3. Specifically, Figures 3a and 3b show the percentages of fibres in MPs and MRs,  
190 respectively, with remaining particles being films and fragments (MR spherules were only  
191 observed at S8, E1), while Figures 3c and 3d show the percentages of fine ( $L \leq 100 \mu\text{m}$ ) particles  
192 in MPs and MRs, respectively, with the majority of remaining particles being large ( $L > 1000$   
193  $\mu\text{m}$ ) at E0 and intermediate ( $L = 100$  to  $1000 \mu\text{m}$ ) above road level. At all locations, there is an  
194 increase in the percentage of fibrous MPs above road level (where the range is 13 to 88%), and  
195 in many cases at one or more of E1, E2 or E3 the entire MP population is made up of fibres. The  
196 percentage of fibrous MRs is considerably lower (and never exceeds 25% overall and 5% at road  
197 level), and in most (but not all) cases, fibres are more abundant at elevation than at road level. At  
198 all locations, the percentage of fine MPs is higher at E1, E2 and E3 than at road level, and while  
199 the distribution of fine MRs is more complex, the highest percentages are usually found at E3.

200 Regarding MP fibre diameter, the overall distribution was: 88.8% thin, 7.9% medium, and 3.3%  
201 thick. At road level, however, there was a greater percentage of thick fibres and a smaller  
202 percentage of thin fibres compared with corresponding values at the remaining elevations, and  
203 thick fibres were completely absent at ten sites at E3.

204

205

206 Figure 3: Percentage of (a) fibres in MPs, (b) fibres in MRs, (c) fine MPs ( $L \leq 100 \mu\text{m}$ ) and (d) fine MRs ( $L \leq 100 \mu\text{m}$ ) at road level  
207 and the different elevations of each sampling location.



209

210 The results of the Raman analysis of selected MPs are shown in Table 3. The most commonly  
211 encountered polymers amongst the fibres analysed ( $n = 21$ ) were polyethylene terephthalate and  
212 nylon, with polypropylene, polyvinylchloride, polyester, chlorinated polyisoprene and  
213 polyurethane also detected. Amongst the fragments analysed ( $n = 9$ ), polyethylene was present in  
214 three cases, with polyethylene terephthalate, polypropylene, nylon and polyvinylchloride also  
215 detected.

216 Table 3: Polymeric composition of MPs analysed by micro-Raman spectrometry ( $n = 30$ ).

polymer	fibres	fragments
polyethylene terephthalate	9	2
polypropylene	2	2
nylon	3	1
polyethylene	0	3
polyvinylchloride	2	1
polyester-epoxy	2	0
chlorinated polyisoprene	2	0
polyurethane	1	0

217

218

#### 219 **4. Discussion**

220 The accumulation of MPs and MRs in the urban setting is likely controlled by many of the  
221 factors that are responsible for the accumulation of urban dusts more generally, including  
222 microclimate, topography, vegetation, surface roughness, the effects of buildings on airflow and  
223 proximity to direct sources (Weber et al., 2014; Mei et al., 2018; Zhao et al., 2018). Local, direct  
224 sources of MPs and MRs in the urban environment include households, offices, artificial turfs,  
225 littering, manufacturing industries, building construction and renovation, waste disposal,  
226 thermoplastic road markings, and traffic (Dris et al., 2016; Wang et al., 2020; Järllskog et al.,  
227 2020; Kitahara and Nakata, 2020; Yukioka et al., 2020), with the latter in the form of vehicle  
228 tires particularly significant for MRs (NIVA, 2020; Fussell et al., 2022). More distant, diffuse  
229 sources represent the aggregation of these and other sources (including agriculture) over a wider  
230 area (Abbasi et al., 2022). The heterogeneity in the abundance and characteristics of MPs and  
231 MRs across the locations and municipal sectors in Shiraz, therefore, reflects variations in the

232 significance of such sources and factors, but overall accumulation is greater than at the control  
233 location where direct sources, including those associated with traffic and industry, are less  
234 important.

235 There is little quantitative information on MPs and MRs in road dusts and comparisons are not  
236 straightforward because of different methodologies involved in sample collection and  
237 processing, the impacts of different climates (and in particular, rainfall) on material accumulation  
238 and dispersal, and different approaches adopted to isolate, define and analyse plastics and  
239 rubbers. For instance, Patchaiyappan et al. (2021) report a mean and standard deviation of MP  
240 concentrations in < 5 mm urban dusts from Chennai of just  $0.23 \pm 0.09$  MP g<sup>-1</sup> following flotation  
241 in saturated NaCl solution (density ~ 1200 kg m<sup>-3</sup>), and while Järllskog et al. (2020) report a  
242 concentration of 2.6 MPs and MRs combined per g of > 100 µm sweepsand from streets in  
243 Gothenburg after flotation in NaCl, this increased to about 10 per g when a denser solution of  
244 saturated NaI (density ~ 1850 kg m<sup>-3</sup>) was employed. By comparison, when pyrolysis-gas  
245 chromatography-mass spectrometry has been used, O'Brien et al. (2021) report selected MPs  
246 (according to polymer type) in street dusts from Queensland up to 5.9 mg MP g<sup>-1</sup>, while  
247 measurements of the MR content of road dusts and roadside PM10 are on the order of a few  
248 percent by weight (Panko et al., 2019; Youn et al., 2021).

249 More directly comparable with the results of the present study are measurements of MP and MR  
250 abundance in road dusts of other cities in Iran where a similar climate is encountered and broadly  
251 common protocols (including identification criteria and size fractionation) have been adopted  
252 and as summarized in Table 4. Thus, the range and medians of MP concentrations are of similar  
253 orders of magnitude for the large cities of Shiraz and Tehran and the smaller coastal cities of  
254 Asaluyeh and Bushehr, but MR concentrations in Shiraz are considerably higher than those  
255 reported for Asaluyeh and Bushehr where traffic intensity is relatively low.

256

257 Table 4: A summary of MP and MR concentrations in road dusts from Iran.



City	MP g <sup>-1</sup>			MR g <sup>-1</sup>			Source
	min	max	median	min	max	median	
Asaluyeh	3.5	515.0	14.8	2.5	88.3	7.1	Abbasi et al. (2019)
Bushehr	21.0	165.8		4.4	78.2		Abbasi et al. (2017)
Shiraz	3.2	181.0	70.2	68.1	978.8	670.6	This study
Tehran	2.9	20.2	6.1				Dehghani et al. 2017

258  
259 While the quantities of MPs and MRs captured by specifically designed sampling devices  
260 (Brahney et al., 2020) or sampled after specific events (Abbasi et al., 2022) can be employed to  
261 estimate depositional fluxes from the atmosphere, net accumulation rates at the street surface are  
262 not necessarily equivalent to this measure, even in the absence of precipitation. This is because  
263 material deposited by the kerbside is subject to resuspension and redistribution through the  
264 action of wind and pedestrians, air disturbance from passing traffic, and capture and  
265 transportation by vehicle tyres (Venkatram, 2000; Adachi and Tainosho, 2004; Cai and Li, 2019;  
266 Rienda and Alves, 2021). Accumulation of MPs and MRs by passive samplers, like the more  
267 sheltered utility pole steps, may provide better estimates of depositional rates because material  
268 captured is subject to fewer interventions (Amato et al., 2012). However, the fixed orientation  
269 and indented structure of these steps also constrain their use in this respect. Nevertheless, the  
270 relative accumulation (or concentration) of MPs and MRs at different elevations may provide  
271 useful information on the transport and potential impacts of these particles in the urban setting.

272 At road level, net accumulation of MPs and MRs reflects the deposition and redistribution of  
273 particles emitted from traffic close to the road and derived from other local (non-traffic) sources  
274 and a more general, urban background. At elevation, general urban particulate deposition and the  
275 redistribution of traffic sources through resuspension assume greater relative significance. At  
276 different elevations (E1, E2 and E3) it would be reasonable to assume that general atmospheric  
277 deposition is the same and that any differences in the quantities and characteristics of particles  
278 arise, therefore, through the resuspension of material at street level. This results in a decrease in  
279 the amount of material (dust) with increasing elevation and a shift in the fractionation of lighter  
280 MPs and MRs on a number, shape and size basis. Specifically, the quantities of MPs and MRs  
281 per g of dust increase up to E1 (1 m) and decrease at E3 (1.77 m) while the proportions of fine  
282 and fibrous MPs and MRs are persistently (and often progressively) higher at elevation  
283 compared with road level. These observations reflect a combination of distance (elevation) from  
284 the road surface and fractionation of the particle properties that govern resuspension, including

285 aerodynamic size and density (Thatcher and Layton, 1995; Rienda and Alvez, 2021). They also  
286 suggest that there is no significant preferential retention of fine MPs and MRs within the  
287 microstructure of the road surface (NIVA, 2020).

288 Overall, the shift in fractionation with elevation is greater for MRs than MPs, suggesting that the  
289 transport of MRs is more limited. Thus, according to median abundances (per g) in Table 2 (and  
290 excluding the control location), the ratio of MRs to MPs is about 10 at E0 and E1, 3.3 at E2, and  
291 1.1 at E3. Although the density of the principal source of urban rubber (tire particles, about 840  
292  $\text{kg m}^{-3}$ ; Li et al., 2004) is lower than that of MPs (between about 900 and 1500  $\text{kg m}^{-3}$  for the  
293 polymers identified in Table 3), this may be increased by the incorporation of road surface  
294 materials on abrasion to 1200 to 1700  $\text{kg m}^{-3}$  (NIVA, 2020; Jung and Choi, 2022). Moreover, the  
295 shape and size of MRs are more constraining on their transportation relative to thin, fibrous MPs,  
296 effects that can be demonstrated by comparing particle settling velocities in air for MRs and MPs  
297 of equal  $L$ .

298 Thus, according to Henn (1996), the Stokesian (or effective spherical) diameter,  $d_s$ , of a fibre of  
299 100  $\mu\text{m}$  in length and a representative, measured diameter,  $d$ , of 5  $\mu\text{m}$  (aspect ratio,  $\beta = L/d$ , of  
300 20):

$$301 \quad d_s \sim (\ln 2\beta)^{1/2} d \quad (1)$$

302 is about 9.6  $\mu\text{m}$  (and, therefore, classified as  $\text{PM}_{10}$ ). For a microplastic density,  $\rho_{\text{MP}}$ , of 1000  $\text{kg}$   
303  $\text{m}^{-3}$ ,  $d_s$  is also equal to an aerodynamic equivalent diameter,  $d_a$ :

$$304 \quad d_a \sim (\rho_{\text{MP}} \ln 2\beta)^{1/2} d \quad (2)$$

305 The settling velocity,  $v_s$ , of such a fibre is given by:

$$306 \quad v_s = (\rho_{\text{MP}} - \rho_{\text{air}}) g d_s^2 / 18\eta \quad (3)$$

307 where  $\rho_{\text{air}}$  is the density of air at 25°C (= 1.17  $\text{kg m}^{-3}$ ) and  $\eta$  is its viscosity (= 18.6 x 10<sup>-6</sup>  $\text{m}^2 \text{s}^{-1}$ ),  
308 and is equal to about 0.0027  $\text{m s}^{-1}$ . For a polymer of density 1500  $\text{kg m}^{-3}$ ,  $v_s$  is about 0.004  $\text{m s}^{-1}$   
309 according to equation 3. By comparison, the settling velocities of fragments of MR of densities,  
310  $\rho_{\text{MR}}$ , 840  $\text{kg m}^{-3}$  and 1200  $\text{kg m}^{-3}$ , and  $d = 100 \mu\text{m}$  can be modelled as quasi-spheres (the mode of  
311 distribution of circularity of tire wear particles is 0.83; Kreider et al., 2010):

312  $v_s = (\rho_{MR} - \rho_{air})gd^2/18\eta$  (4)

313 resulting in settling velocities of about 0.25 m s<sup>-1</sup> and 0.35 m s<sup>-1</sup>, respectively. Despite  
314 uncertainties regarding fragment shape, a difference in  $v_s$  of two orders of magnitude between the  
315 two particle types illustrates the greater mobility and susceptibility for atmospheric transport for  
316 urban MP fibres relative to urban MR fragments.

317 Qualitatively, these observations and calculations are consistent with findings in the literature.  
318 For example, Pandey et al. (2022) found that while fragments dominated the MP population on  
319 the street of an Indian city, fibres dominated MPs in the atmosphere at an elevation of 7.5 m.  
320 Panko et al. (2013) showed that < 1% of PM<sub>10</sub> sampled at 1.5 to 2.5 m above the ground in  
321 various urbanised districts in the US, Europe and Japan was made up of tire and road wear  
322 particles, suggesting that the majority of fine MRs remain at road level.

323 The direct and indirect impacts of airborne MPs and MRs on human health are unclear, and in  
324 particular at realistic levels of exposure (Abbasi et al., 2019; Fussell et al., 2022). However, they  
325 are likely to depend on factors such as size, shape, polymeric composition and the nature and  
326 availability of any additives or chemicals acquired from the environment (Amato-Lourenço et  
327 al., 2020; Vethaak and Legler, 2020). Nevertheless, in terms of exposure in the urban setting, the  
328 present study is significant in demonstrating fractionation of characteristics of MPs and MRs that  
329 are believed to be critical to respiratory health through an elevation of less than 2 m. Thus, at  
330 1.77 m (E3), representative of the height of an adult, particles are less abundant (relative to other  
331 solids), more fibrous (at least for MPs) and finer and thinner than those at 1 m (E2),  
332 representative of the height of a young child. That is, children might be exposed to more MPs  
333 and MRs through inhalation than adults, but these particles are likely to be coarser and less  
334 fibrous.

## 335 **5. Conclusions**

336 In different municipal sectors throughout the city of Shiraz, the accumulation of roadside dusts,  
337 MPs and MRs were spatially heterogeneous. However, and regardless of location, all types of  
338 solid exhibited a decline in accumulation, and MPs and MRs showed a decrease in concentration  
339 (per g of dust), with increasing elevation up to about 1.8 m. Increasing elevation was also  
340 associated with a reduction in particle size and percentage of fibres, and in particular for MPs.

341 The fractionation of MPs and MRs by height is attributed to the resuspension of material by wind  
342 and passing traffic and results in exposure scenarios for adults and children in the urban setting  
343 that are subtly, but potentially significantly, different.

344

#### 345 **Acknowledgements**

346 We thank Shiraz University for funding this research.

347

#### 348 **References**

349 Abbasi, S., Keshavarzi, B., Moore, F., Delshab, H., Soltani, N. & Sorooshian, A. 2017.

350 Investigation of microrubbers, microplastics and heavy metals in street dust: a study in Bushehr  
351 city, Iran. *Environmental Earth Sciences*, 76, 1-19.

352 Abbasi, S., Keshavarzi, B., Moore, F., Turner, A., Kelly, F. J., Dominguez, A. O. & Jaafarzadeh,  
353 N. 2019. Distribution and potential health impacts of microplastics and microrubbers in air and  
354 street dusts from Asaluyeh County, Iran. *Environmental pollution*, 244, 153-164.

355 Abbasi, S., Rezaei, M., Ahmadi, F. & Turner, A. 2022. Atmospheric transport of microplastics  
356 during a dust storm. *Chemosphere*, 292, 133456.

357 Adachi, K., Tainosho, Y., 2004. Characterization of heavy metal particles embedded in tire dust.  
358 *Environment International* 30, 1009-1017.

359 Alvez, C.A., Vicente, E.D., Vicente, A.M.P., Rienda, I.C., Tomé, M., Querol, X., Amato, F.,  
360 2020. *Science of the Total Environment* 737, 139596.

361 Amato, F., Karanasiou, A., Moreno, T., Alastuey, A., Orza, J.A.G., Lumbreras, J., Borge, R.,  
362 Boldo, E., Linares, C., Querol, X., 2012. Emission factors from road dust resuspension in a  
363 Mediterranean freeway. *Atmospheric Environment* 61, 580-587.

364 Amato-Lourenço, L.F., dos Santos Galvão, L., de Wager, L.A., Hiemstra, P.S., Vijver, M.G.,  
365 Mauad, T., 2020. An emerging class of air pollutants: Potential effects of microplastics to  
366 respiratory human health? *Science of the Total Environment* 749, 141676.

367 Brahney, J., Hallerud, M., Heim, E., Hahnenberger, M., Sukumaran, S., 2020. Plastic rain in  
368 protected areas of the United States. *Science* 368, 1257-1260.

369 Cai, K., Li, C., 2019. Street dust heavy metal pollution source apportionment and sustainable  
370 management in a typical city - Shijiazhuang, China. *Int. J. Res. Public Health* 16, 2625.

371 Dehghani, S., Moore, F., Akhbarizadeh, R., 2017. Microplastic pollution in deposited urban dust,  
372 Tehran metropolis, Iran. *Environmental Science and Pollution Research*. DOI 10.1007/s11356-  
373 017-9674-1

374 Dris R, Gasperi J, Saad M, Mirande C, Tassin B (2016) Synthetic fibers in atmospheric fallout: a  
375 source of microplastics in the environment? *Mar. Pollut. Bull.* 104, 290–293.

376 Escrig, A., Amato, F., Pandolfi, M., Monfort, E., Querol, X., Celades, I., Sanf elix, V., Alastuey,  
377 A., Orza, J.A.G., 2011. Simple estimates of vehicle-induced resuspension rates. *Journal of*  
378 *Environmental Management* 92, 2855-2859.

379 Fussell JC, Franklin M, Green DC, Gustafsson M, Harrison RM, Hicks W, Kelly FJ, Kishta F,  
380 Miller MR, Mudway IS, Oroumihyeh F, Selley L, Wang M, Zhu Y., 2022. A review of road  
381 traffic-derived non-exhaust particles: emissions, physicochemical characteristics, health risks,  
382 and mitigation measures. *Environ Sci Technol.* 56, 6813-6835.

383 Henn, A.R., 1996. Calculation of the Stokes and Aerodynamic Equivalent Diameters of a Short  
384 Reinforcing Fiber. *Particle and Particle Systems Characterization* 13, 249-253.

385 J rllskog, I., Str mwwall, A.M., Magnusson, K., Gustafsson, M., Polukarova, M., Galfi, H.,  
386 Aronsson, M., Andersson-Sk ld, Y., 2020. Occurrence of tire and bitumen wear microplastics on  
387 urban streets and in sweepsand and washwater. *Sci. Total Environ.* 729, 138950.

388 Jung, U., Choi, S.S., 2022. Classification and characterization of tire-road wear particles in road  
389 dust by density. *Polymers* 14, 10.3390/polym14051005

390 Kitahara, K.I., Nakata, H., 2020. Plastic additives as tracers of microplastic sources in Japanese  
391 road dusts. *Science of the Total Environment* 736, 139694.

392 Kreider M. L., Panko, J.M., McAtee, B.L., Sweet, L.I., Finley, B.L., 2010. Physical and chemical  
393 characterization of tire-related particles: Comparison of particles generated using different  
394 methodologies. *Science of the Total Environment* 408, 652-659.

395 Kuenen, J.J.P., Visschedijk, A.J.H., Jozwicka, M., Denier van der Gon, H.A.C., 2014. TNO-  
396 MACC\_II emission inventory; a multi-year (2003e2009) consistent high resolution European  
397 emission inventory for air quality modeling. *Atmos.Chem. Phys.* 14, 10963-10976.

398 Li, G., Stubblefield, M.A., Garrick, G., Eggers, J., Abadie, C., Huang, B., 2004. Development of  
399 waste tire modified concrete. *Cement and Concrete Research* 34, 2283-2289.

400 Liu, K., Wu, T., Wang, X., Song, Z., Zong, C., Wei, N., Li, D., 2019. Consistent transport of  
401 terrestrial microplastics to the ocean through atmosphere. *Environmental Science and*  
402 *Technology* 53, 10612-10619.

403 Mei, D., Wen, M., Xu, X., Zhu, Y., Xing, F., 2018. The influence of wind speed on airflow and  
404 fine particle transport within different building layouts of an industrial city. *Journal of the Air*  
405 *and Waste Management Association* 68, 1038-1050.

406 Moskovchenko, D.; Pozhitkov, R.; Soromotin, A.; Tyurin, V., 2022. The content and sources of  
407 potentially toxic elements in the road dust of Surgut (Russia). *Atmosphere* 13, 30  
408 <https://doi.org/10.3390/atmos13010030>

409 NIVA, 2020. Microplastics in road dust – characteristics, pathways and measures. Report SNO  
410 7526-2020, Norwegian Institute for Water Research (NIVA), Oslo.

411 O'Brien, S., Okoffo, E.D., Rauert, C., O'Brien, J.W., Ribeiro, F., Burrows, S.D., Toapanta, T.,  
412 Wang, X., Thomas, K.V., 2021. Quantification of selected microplastics in Australian urban road  
413 dust. *Journal of Hazardous Materials* 416, 125811.

414 Pandey, D., Banerjee, T., Badola, N., Chauhan, J.S., 2022. Evidences of microplastics in aerosols  
415 and street dust: a case study of Varanasi City, India. *Environmental Science and Pollution*  
416 *Research* <https://doi.org/10.1007/s11356-022-21514-1>

417 Panko, J.M., Chu, J., Kreider, M.L., Unice, K.M., 2013. Measurement of airborne concentrations  
418 of tire and road wear particles in urban and rural areas of France, Japan, and the United States.  
419 *Atmospheric Environment* 72, 192-199.

420 Panko, J.M., Hitchcock, K.M., Fuller, G.W., Green, D., 2019. Evaluation of tire wear  
421 contribution to PM<sub>2.5</sub> in urban environments. *Atmosphere* 10, 99; doi:10.3390/atmos10020099.

422 Rienda, I.C., Alves, C.A., 2021. Road dust resuspension: A review. *Atmospheric Research* 261,  
423 105740.

424 Rogge, W.F., Hildemann, L.M., Mazurek, M.A., Cass, G.R., 1993. Sources of fine organic  
425 aerosol. 3. Road dust, tire debris, and organometallic brake lining dust: Roads as sources and  
426 sinks. *Environ. Sci. Technol.* 27, 1892-1904.

427 Thatcher, T.L., Layton, D.W., 1995. Deposition, resuspension, and penetration of particles  
428 within a residence. *Atmospheric Environment* 29, 1487-1497.

429 Thorpe, A., Harrison, R.M., 2008. Sources and properties of non-exhaust particulate matter from  
430 road traffic: a review. *Sci. Total Environ.* 400, 270-282.

431 Thouron, L., Seigneur, C., Kim, Y., Mahé, F., André, M., Lejri, D., Villegas, D., Bruge, B.,  
432 Chanut, H., Pellan, Y., 2018. Intercomparison of three modeling approaches for traffic-related  
433 road dust resuspension using two experimental data sets. *Transportation Research Part D*, 58,  
434 108-121.

435 Venkatram, A., 2000. A critique of empirical emission factor models: a case study of the AP-42  
436 model for estimating PM<sub>10</sub> emissions from paved roads. *Atmospheric Environment* 34, 1-11.

437 Vethaak, A.D., Legler, J., 2020. Microplastics and human health - knowledge gaps should be  
438 addressed to ascertain the health risks of microplastics. *Science* 371, 672-674.

439 Wagner, J., Leith, D., 2001. Passive aerosol sampler. Part I: Principle of operation. *Aerosol Sci.*  
440 *Technol.* 34, 186-192.

441 Wang, Q., Enyoh, C.E., Chowdury, T., Chowdury, M.A.H., 2020. Analytical techniques,  
442 occurrence and health effects of micro and nano plastics deposited in street dust. *Int. J. Environ.*  
443 *Anal. Chem.* <https://doi.org/10.1080/03067319.2020.1811262>

444 Weber, F., Kowarik, I., Säumel, I., 2018. Herbaceous plants as filters: Immobilization of  
445 particulates along urban street corridors. *Environmental Pollution* 186, 234-240.

446 Weinbruch, S., Worringen, A., Ebert, M., Scheuven, D., Kandler, K., Pfeffer, U., Bruckmann,  
447 P., 2014. A quantitative estimation of the exhaust, abrasion and resuspension components of  
448 particulate traffic emissions using electron microscopy. *Atmospheric Environment* 99, 175-182.

449 Youn, J.S., Kim, Y.M., Siddiqui, M.Z., Watanabe, A., Han, S., Jeong, S., Jung, Y.W., Jeon, K.J.,  
450 2021. Quantification of tire wear particles in road dust from industrial and residential areas in  
451 Seoul, Korea. *Science of the Total Environment* 784, 147177.

452 Yukioka, S., Tanaka, S., Nabetani, Y., Suzuki, Y., Ushijima, T., Fujii, S., Takada, H., Tran,  
453 Q.V., Singh, S., 2020. Occurrence and characteristics of microplastics in surface road dust in  
454 Kusatsu (Japan), Da Nang (Vietnam), and Kathmandu (Nepal). *Env. Pollut.* 256, 113447.

455 Zhao, H., Jiang, Q., Xie, W., Li, X., Yin, C., 2018. Role of urban surface roughness in road-  
456 deposited sediment build-up and wash-off *Journal of Hydrology* 560, 75-85.

457

458

459

460

461

462

463

464